British Journal of Pharmacology

DOI:10.1111/bph.13263
www.brjpharmacol.org

RESEARCH PAPER

Simulating the influence of plasma protein on measured receptor affinity in biochemical assays reveals the utility of Schild analysis for estimating compound affinity for plasma proteins

D Blakeley[3], D A Sykes[1], P Ensor[1], E Bertran[4], P J Aston[2] and S J Charlton[1]

[1]School of Life Sciences, University of Nottingham, Nottingham, UK, [2]Department of Mathematics, University of Surrey, Guildford, UK, [3]Novartis Institutes for Biomedical Research, Horsham, West Sussex, UK, and [4]Roche Innovation Center Basel, Switzerland

Correspondence
Steven J. Charlton, School of Life Sciences, Queen's Medical Centre, University of Nottingham, Nottingham, NG7 2UH, UK.
E-mail: steven.charlton@nottingham.ac.uk

Received
30 May 2013
Revised
16 July 2015
Accepted
17 July 2015

BACKGROUND AND PURPOSE

Plasma protein binding (PPB) influences the free fraction of drug available to bind to its target and is therefore an important consideration in drug discovery. While traditional methods for assessing PPB (e.g. rapid equilibrium dialysis) are suitable for comparing compounds with relatively weak PPB, they are not able to accurately discriminate between highly bound compounds (typically >99.5%). The aim of the present work was to use mathematical modelling to explore the potential utility of receptor binding and cellular functional assays to estimate the affinity of compounds for plasma proteins. Plasma proteins are routinely added to *in vitro* assays, so a secondary goal was to investigate the effect of plasma proteins on observed ligand–receptor interactions.

EXPERIMENTAL APPROACH

Using the principle of conservation of mass and the law of mass action, a cubic equation was derived describing the ligand–receptor complex [*LR*] in the presence of plasma protein at equilibrium.

KEY RESULTS

The model demonstrates the profound influence of PPB on *in vitro* assays and identifies the utility of Schild analysis, which is usually applied to determine receptor-antagonist affinities, for calculating affinity at plasma proteins (termed K_P). We have also extended this analysis to functional effects using operational modelling and demonstrate that these approaches can also be applied to cell-based assay systems.

CONCLUSIONS AND IMPLICATIONS

These mathematical models can potentially be used in conjunction with experimental data to estimate drug-plasma protein affinities in the earliest phases of drug discovery programmes.

Abbreviations

HSA, human serum albumin; IC_{50}, drug concentration required to give a 50% inhibition of either radioligand binding or functional response; K_d, equilibrium dissociation constant of drug for receptor; K_E, the concentration of agonist–receptor complex that elicits 50% maximal response; K_P, equilibrium dissociation constant of drug for plasma protein (human serum albumin); K_R, equilibrium dissociation constant of drug for receptor (used in the model); RED, rapid equilibrium dialysis; RO-1138452 4,5-dihydro-N-[4-[[4-(1-methylethoxy) phenyl]methyl]phenyl]-1H-imadazol-2-amine, (aprostacyclin IP receptor antagonist)

© 2015 The British Pharmacological Society

Tables of Links

TARGETS
IP receptor

LIGANDS
RO-1138452

These Tables list key protein targets and ligands in this article which are hyperlinked to corresponding entries in http://www.guidetopharmacology.org, the common portal for data from the IUPHAR/BPS Guide to PHARMACOLOGY (Pawson *et al.*, 2014) and are permanently archived in the Concise Guide to PHARMACOLOGY 2013/14 (Alexander *et al.*, 2013).

Introduction

In vivo drug molecules may be considered to be either bound to proteins and lipids in plasma and tissue or free to diffuse in the aqueous environment that surrounds them. The binding of drugs to plasma protein, mainly to α-acid glycoprotein and serum albumin, can have a profound effect on the activity of a drug and is crucially involved in dictating drug pharmacokinetic and pharmacodynamic relationships. Human serum albumin (HSA) is the most abundant extracellular protein found in blood plasma and tissue fluids (M_r 66 kDa, 0.53–0.75 mM, Goodman & Gilman 1996) and is by far the most important non-specific transporter protein in the circulatory system. HSA acts as a transporter molecule for a variety of endogenous compounds including nutrients such as fatty acids, hormones and waste products including haem, bilirubin and a range of renal toxins. This one protein is able to bind a variety of structurally diverse naturally occurring ligands and can also bind to a wide range of drug molecules. This ability of albumin to adsorb a significant amount of drug in plasma and tissue fluids is the basis of the pharmaceutical industry's long-standing interest in the protein. According to the 'free drug hypothesis', the pharmacological activity or effectiveness of a drug will be determined by the exposure to the unbound concentration of that drug in plasma rather than its total concentration (Trainor 2007). As a consequence, drugs that show high plasma protein binding will require dosing at higher concentrations in order to achieve their therapeutic effect. This is often in spite of the fact that the affinity of the drug is higher for the receptor or enzyme target and is a direct consequence of the high concentration of albumin present in blood plasma. It is important to note, however, that drug-protein binding not only affects the binding of drug to a receptor but also affects the rate at which drugs are eliminated from the body, prolonging exposure of certain compounds. For these reasons, pharmaceutical companies have developed screens for HSA binding early in the drug discovery process to better understand these complex interactions.

Traditionally, plasma protein binding is assessed by equilibrium dialysis and ultrafiltration methods that define the fraction or percentage of compound that is protein bound and free in solution. Such methods provide good quantification of serum protein binding for many compounds but can be of limited utility in discriminating between highly bound compounds that can have affinities in the nM range (Kratochwil *et al.*, 2002). The usual limit of accurate detection is defined as >99.5%, but it is not uncommon for whole chemical series to display this level of plasma protein binding. This makes it difficult to distinguish between compounds based on plasma protein binding and offers little information about the structure–activity relationship for plasma protein binding. This situation can be illustrated using the model described by Toutain and Bousquet-Melou (2002). By formulating expressions for the free fraction of drug in terms of free and total plasma concentrations as well as incorporating the principle of conservation of drug, an equation with some underlying assumptions is derived for the free fraction of drug, namely $fu = K_P/(B_{max} + K_P)$, where K_P and B_{max} are the protein affinity and maximal binding capacity constants for the protein. Using the previous equation, the % of ligand unbound can be readily calculated for a protein concentration or B_{max} equal to 600 μM (or 4% HSA) (Table 1, with corresponding Figure 1). This highlights the fact that strongly bound compounds are represented by a very narrow interval on the percentage scale, and measurements made here are therefore more prone to error. This can be overcome, in part, by performing dilutions of plasma, but this can result in limitations with accurately quantifying drug concentrations.

As serum protein can be readily included in an *in vitro* pharmacology assay, it should be possible to calculate the degree of compound binding to plasma protein by observing the changes in observed affinity in the presence of plasma protein, using so-called serum-shift assays. The

Table 1

The relationship between the % plasma protein binding and binding affinity

Drug K_P for protein (μM)	% plasma protein unbound	Estimated unbound (drug) (μM)	% plasma protein binding
0.001	0.00017	0.000017	99.9998
0.01	0.00167	0.000167	99.9983
0.1	0.01666	0.001666	99.9833
1	0.16639	0.016639	99.8336
10	1.63934	0.163934	98.3607
100	14.28571	1.428571	85.7143
1000	62.50000	6.250000	37.5000

% unbound based on the formula provided by Toutain and Bousquet-Melou (2002) $fu = K_P/(B_{max} + K_P)$, assuming a B_{max} or protein concentration of 600 μM. Unbound drug concentration was calculated based on the addition of 10 μM drug to plasma protein.

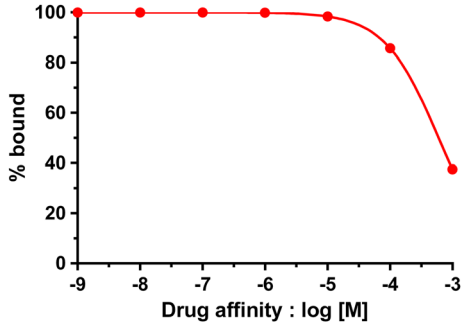

Figure 1

Graphical representation of the relationship between % plasma protein binding and protein binding affinity. For simulation purposes, the total concentration of ligand ($[L]_T$) was fixed at 10 μM, and the total plasma protein concentration was fixed at 600 μM.

measurement of apparent K_d values for serum protein by IC_{50} shift analysis has been explored previously (Copeland, 2000; Rusnak *et al.*, 2004). Copeland and colleagues have presented a practical and theoretical treatment of the relationship between the IC_{50} determined by *in vitro* assays in the presence and absence of plasma proteins and the apparent K_d value for ligand binding to protein. These mathematical approaches, albeit in an enzymology context, have provided the experimenter with a practical way of calculating affinity values of unlabelled compounds.

In this study, we have expanded upon the models of Copeland and Rusnak to include the conservation of all three binding partners, namely ligand, protein and receptor, producing explicit mathematical solutions that can be applied to experimental data (both binding and functional) to provide estimates of K_P This analysis allows the investigator to determine K_P values for both labelled ligands using the technique of saturation binding and also for unlabelled agonists in functional assays using 'operational model' fitting. Finally, we also demonstrate that a Schild analysis-type approach can provide the investigator with a relatively simple method to estimate drug-protein affinities. Such information may be used to better understand the structural determinants of plasma protein binding.

Methods

Mathematical model

We consider a simple model in which the radioligand binds to both receptor and protein according to the law of mass action and in which the conservation of mass applies. The model consists of two binding processes, as illustrated below:

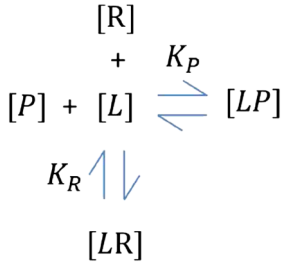

where $[L]$, $[R]$ and $[P]$ denote (free) radioligand, (free) receptor and (free) protein concentrations, respectively, $[LR]$ and $[LP]$ are ligand–receptor and ligand–protein complex concentrations, respectively, and K_R and K_P are their associated equilibrium dissociation constants. All concentrations are measured in units of molar unless otherwise stated. The equilibrium equations for the above processes are given by:

$$k_{R+}[L][R] - k_{R-}[LR] = 0$$
$$k_{P+}[L][P] - k_{P-}[LP] = 0$$

where k_{R+}, k_{R-}, k_{P+} and k_{P-} are the association and dissociation rates of ligand binding to receptor and protein. These relations can be expressed as:

$$[L][R] = K_R[LR] \quad (1)$$

$$[L][P] = K_P[LP] \quad (2)$$

where $K_R = \frac{k_{R-}}{k_{R+}}$ and $K_P = \frac{k_{P-}}{k_{P+}}$. Additionally, from the conservation of mass principle, we have the following simple equations:

$$[L]_T = [L] + [LR] + [LP] \quad (3)$$

$$[P]_T = [P] + [LP] \quad (4)$$

$$[R]_T = [R] + [LR] \quad (5)$$

where $[L]_T$ is the total concentration of ligand added, $[P]_T$ the total concentration of protein added and $[R]_T$ the total concentration of receptor added. This gives five equations in the five unknowns $[L]$, $[R]$, $[P]$, $[LR]$ and $[LP]$ which, in combination, can be used to describe the three interacting components at equilibrium. By suitable rearrangements of Equations (1) to (5), further equations describing the concentrations of ligand bound to both protein and receptor may be formulated, and these two equations can be further reduced to a single cubic equation in the variable $[LR]$. To see this, we rearrange Equations 3–5 so that the free concentrations of ligand, protein and receptor are expressed in terms of the total concentrations plus complex concentrations, for example, $[L]_T - [LR] - [LP] = [L]$, and insert these into Equations (1) and (2), which leads to the following relationships:

$$K_R[LR] - \left([L]_T - [LR] - [LP]\right)\left([R]_T - [LR]\right) = 0) \quad (6)$$

$$K_P[LP] - \left([L]_T - [LR] - [LP]\right)\left([P]_T - [LP]\right). = 0 \quad (7)$$

Solving 6 for $[LP]$ yields

$$[LP] = \frac{1}{[LR] - [R]_T}\left(K_R[LR] - [L]_T[R]_T + [L]_T[LR] + [LR][R]_T - [LR]^2\right) \quad (8)$$

(See Appendix 1 for a mathematical discussion on the validity of this expression.)

Insertion of the expression for [*LP*] in Equation 8 into 7 yields a cubic equation in terms of [*LR*], namely

$$A[LR]^3 + B[LR]^2 + C[LR] + D = 0 \quad (9)$$

where

$$A = K_R - K_P$$
$$B = K_P K_R + 2\,K_P[R]_T + K_P[L]_T + K_R[P]_T - K_R^2 - K_R[L]_T - K_R[R]_T$$
$$C = [R]_T(-K_P K_R - K_P[R]_T - 2\,K_P\,[L]_T - K_R[P]_T + K_R[L]_T)$$
$$D = K_P[L]_T[R]_T^2$$

A cubic equation can be solved using Cardano's method (Weisstein), a derivation of which is given in Appendix 2. We also show in Appendix 2 that the cubic equation 9 has a single solution satisfying $0 \le [LR] < [R]_T$ and that this is the solution that is relevant for this problem. It is found numerically that the cubic equation has three real roots, and the required solution of the equation is given by:

$$[LR] = 2\sqrt{\frac{-q}{3}}\cos\left(\frac{\theta + 2\pi}{3}\right) - \frac{a}{3} \quad (10)$$

where the parameters a, θ and q are related to the parameters K_R, K_P, $[L]_T$, $[R]_T$, and $[P]_T$ using the expressions given in Appendix 2. This solution is also presented in GraphPad PRISM language in Appendix 2. With an explicit solution for the ligand–receptor complex formulated, we now proceed to show how varying these parameters affects the observed profile of ligand–receptor saturation plots and concentration–response curves.

[^{3}H]-RO-1138452 saturation binding

The saturation binding assays were performed in 96-deep-well plates at room temperature (~21°C). A range of concentrations of [^{3}H]-RO-1138452 were used in the assay (~5 pM–10 nM) in order to construct saturation binding curves as described by Sykes *et al.*, 2009. CHO-IP cell membranes (2.5 μg per well) were incubated in binding buffer containing 20 mM HEPES, 10 mM $MgCl_2$ and 0.02% (w v^{-1}) pluronic acid, with continuous gentle agitation for 2.5 h to ensure equilibrium was reached. The assay was performed in the presence of a range of concentrations of HSA (0–640 μM). To avoid ligand depletion at the low concentrations of [^{3}H]-RO-1138452 used in the assay, the assay volume was increased to 1.5 mL. Non-specific binding was determined using 1 μM unlabelled RO-1138452. After incubation, the bound and free [^{3}H]-RO-1138452 were separated by rapid vacuum filtration using a FilterMate Cell Harvester (Perkin Elmer, Waltham, USA) onto 96-well GF/C filter plates and rapidly washed three times with ice-cold wash buffer (20 mM HEPES, 1 mM $MgCl_2$ and pH 7.4). After drying (>4 h), 40 μL of Microscint-20 (Perkin Elmer) was added to each well. Radioactivity was quantified using single-photon counting on a TopCount microplate scintillation counter (Beckman Coulter, Pasadena, USA). Aliquots of [^{3}H]-RO-1138452 were also quantified accurately to determine how much radioactivity was added to each well using liquid scintillation spectrometry on an LS6500 scintillation counter (Beckman Coulter).

As the amount of radioactivity varied slightly for each experiment (<5%), data are expressed graphically as the mean ± range for individual representative experiments unless otherwise stated, whereas all values reported in the text and tables are mean ± SEM for at least three separate experiments. Concentration–response data were also fitted using a four-parameter logistic equation. Statistical analysis performed and data fitting were performed using Prism software (ver. 5.03; GraphPad Software, San Diego, USA).

Rapid equilibrium dialysis

Rapid equilibrium dialysis (RED) was performed as described by Waters *et al.* (2008) using a 48-cell RED device manufactured by Pierce Biotechnology (Thermo Fisher Scientific, Waltham, USA). Briefly, RO-1138452 was incubated with human plasma at a concentration of 5 μM for 10 min after which it was transferred (200 μL) to one of the two sample chambers in the RED device. Three hundred and fifty microlitres of 100 mM phosphate buffer was added to the adjacent chamber, the plate was sealed and the system was left to equilibrate on a shaker at 37°C for 4 h. Fifty microlitres of each sample was transferred to a new 96-well plate and diluted with 50 μL of phosphate buffer. Two hundred fifty microlitres of acetonitrile containing IS (sulfadimethoxine, 0.1 μg mL^{-1}) was added to the wells, the plate was centrifuged (room temperature, 1000 g, 10 min), and 150 μL of supernatant was transferred into a fresh 96-well plate and diluted with 150 μL of deionized water. Chromatographic separation was achieved by a Waters Aquity ultraperformance LC (UPLC) system using formic acid (0.1%) as mobile phase A and methanol as mobile phase B. The UPLC column was a Waters Acquity BEH, 1.9 μm, 2.1 × 50 mm. Under the described conditions, the retention time of RO-1138452 was 1.2 min. Detection was performed by an Applied Biosystems (Carlsbad, USA) API5500 mass spectrometer with turbo ion spray ionization in positive mode, and RO1138452 quantified using area of the chromatographic peak divided by that of the internal standard to obtain the area peak ratio. The peak area ratio corresponding to the buffer side was divided by that corresponding to the plasma side in each RED device, to calculate the percentage of free drug. This was carried out for the three replicates of each experiment, and a mean and coefficient of variation were calculated.

Results

Simulations of ligand–receptor [LR] binding curves

In these simulations, the concentration of total ligand added was varied, and the concentration of ligand–receptor complex formed was plotted for a given set of parameter values relevant to *in vitro* studies. Simulations were performed using Microsoft Excel version 10 and Maple version 11 and graphically illustrated using GraphPad Prism 5.0.

Effect of plasma protein on apparent binding affinity. The effect of increasing receptor affinity K_R on the concentration of ligand–receptor binding complex formed is shown in

Figure 2A, a simulation performed in the absence of plasma protein, that is $[P]_T = 0$. A typically encountered receptor concentration $[R]_T$ was employed fixed at 0.1 nM, and total ligand added $[L]_T$ ranged from 0.03 pM to 100 μM. As the affinity of the ligand for the receptor was decreased, the receptor occupancy curves shifted to the right, as one would predict. Of particular note in the figure is the concept of ligand depletion, a phenomenon most evident experimentally when using high-affinity ligands in assay systems where binding of ligand to receptor results in a significant reduction in the free ligand concentration (Wells *et al.*, 1980; Goldstein & Barrett, 1987; Carter *et al.* 2007). For ligand affinities $K_R \leq 0.1$ nM where the concentration of receptor exceeds the concentration of added ligand by >10-fold, ligand depletion results in saturation plots from which inaccurate estimates of K_R will be determined. It is also apparent from Figure 2A how ligand depletion results in saturation binding curves that have much steeper gradients as also evident in Carter *et al.* (2007).

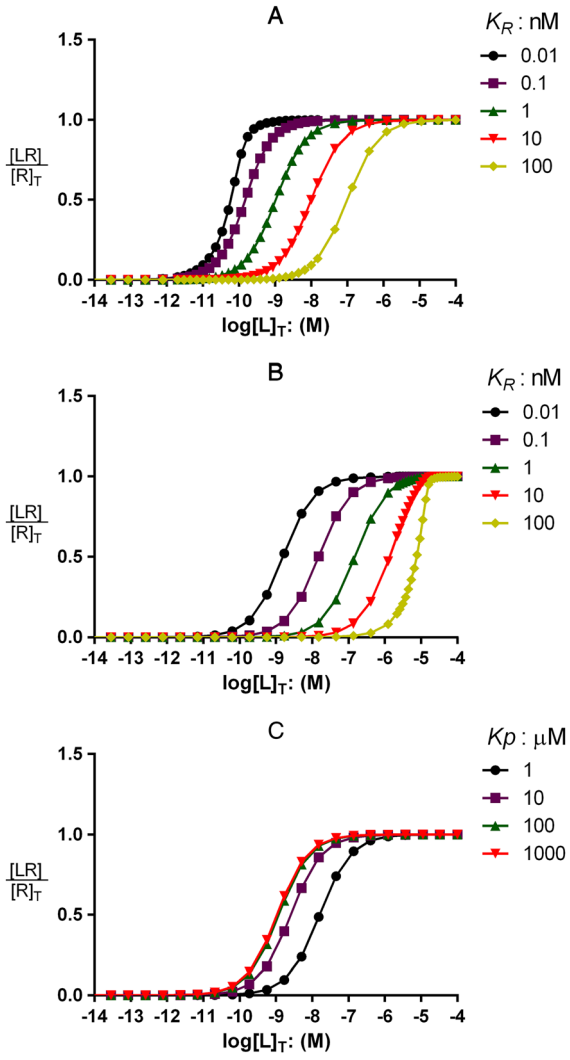

Figure 2

Ligand–receptor occupancy simulations. (A) Simulation of the effect of decreasing receptor–ligand affinity on the concentration of ligand bound to receptor in the absence of plasma protein. (B) Simulation of the effect of decreasing receptor–ligand affinity on the concentration of ligand bound to receptor in the presence of plasma protein. The affinity of the ligand (K_P) for the protein in this simulation is 0.1 μM with the total concentration of protein added $[P]_T$ fixed at 15 μM (0.1%). (C) Simulation of the effects of decreasing ligand–protein affinity K_P on the concentration of ligand bound to receptor. In this simulation, the total concentration of plasma protein ($[P]_T$) added was 15 μM, and the affinity for the receptor was $K_R = 1$ nM. In all the above simulations, the total receptor concentration $[R]_T$ was fixed at 0.1 nM.

The direct effect of including protein, $[P]_T = 15$ μM, $K_P = 0.1$ μM in the model is illustrated in Figure 2B. For the same parameter values of $[R]_T$ and K_R employed to produce Figure 2A, a parallel rightward shift of the receptor occupancy curve is now evident in the presence of plasma protein. The apparent K_R observed in the presence of protein is shifted ~100-fold from the actual value of K_R obtained in its absence. Saturation of protein by ligand is now evident when one considers affinities at the receptor of $K_R \geq 100$ nM, under these conditions as ligand concentration is increased, a disproportionate concentration of ligand becomes freely available to bind receptors (i.e. a deviation from constant % fraction unbound).

The final figure in this trilogy, Figure 2C, illustrates the effect of changing drug affinity K_P for a fixed concentration of protein (15 μM or 0.1%), a concentration routinely employed in receptor binding and functional assays. Decreasing the affinity of the ligand for the protein results in ligand–receptor $[LR]$ binding curves resembling standard saturation plots without protein from which the true affinity of the ligand for its receptor can be estimated.

Simulations of protein-bound drug and free drug. Equation (8) can be used to find the concentration of ligand bound to protein $[LP]$ from which one can derive the concentration of free ligand $[L]$ using Equation 3. Figure (3) is an example simulation illustrating the concentration of ligand–protein complex formed at different concentrations of total ligand added for given K_P values. In the simulation, the following parameter values remain fixed $P_T = 15$ μM, $K_R = 1$ nM and $[R]_T = 0.1$ nM. Note again the phenomenon of ligand depletion in situations where protein concentration is in excess of added ligand concentration. As expected,

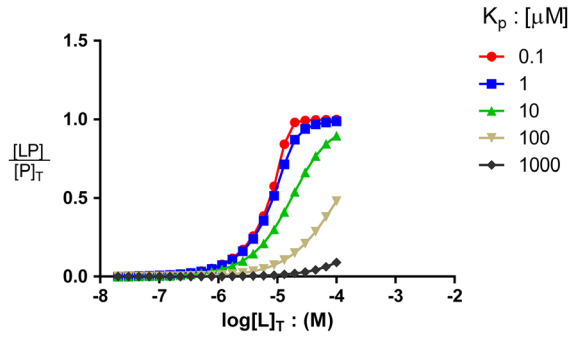

Figure 3

Ligand–protein occupancy simulations. Simulation of the effects of decreasing affinity of ligand for plasma protein K_P on the concentration of ligand bound to plasma protein. In the simulations, $[P]_T = 15$ μM, $K_R = 1$ nM and $[R]_T = 0.1$ nM.

decreasing the affinity of the drug for the protein results in reduced protein occupancy for any given concentration of ligand added. Figure 4 is a plot of the free concentration of ligand against total ligand added on a log–log scale for increasing concentrations of protein. In the simulation, the following parameter values remain fixed: $K_P = 1\,\mu M$, $K_R = 1$ nM and $[R]_T = 0.1$ nM. It was observed that free fraction remains linear up to the point where protein effectively starts to run out, at which point deviations in free ligand occur until eventually the protein saturates and added ligand concentration approximates to free ligand concentration. From an *in vitro* assay perspective, inclusion of 0.1% HSA (or 15 μM) results in an approximately linear relationship between free ligand and total added ligand for concentrations of added ligand $[L]_T < 10\,\mu M$. This linear relationship is the basis of the free fraction calculation employed routinely to estimate free drug concentrations *in vivo* and is based on the % of drug bound to plasma proteins, which can be assumed to be a constant proportion of the total added drug provided that the protein is not fully saturated.

One can formulate cubic equations, similar to that exemplified by Equation (9), describing the ligand–protein complex and free ligand concentrations completely separately and produce explicit cubic solutions as shown in Equation 10. The reader can find full details in Appendix 3. Using the explicit solution given for the concentration [*LR*] in Equation 10 and the resultant concentrations [*L*] and [*LP*], it is instructive to plot these variables in one figure to see visually where the ligand is located for any given concentration of ligand added, as alluded to previously. Figure 5 encapsulates this information in plots of ligand–receptor and ligand–protein occupancy for varying concentrations of ligand added for a ligand with high affinity (1 μM, Figure 5A) and low affinity (100 μM, Figure 5B) for plasma protein. The following parameter values were kept constant $[P]_T = 15\,\mu M$, $K_R = 1$ nM and $[R]_T = 0.1$ nM in both figures.

From Figure 5A, it is apparent that one only has full saturation of both receptor and protein as $[L]_T$ approaches 10 μM,

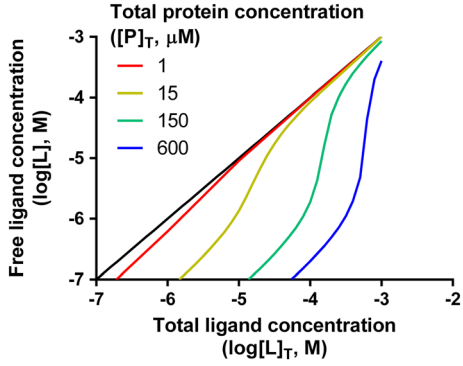

Figure 4

Free ligand predictions with varying plasma protein concentrations. Simulation of the effects of increasing plasma protein concentration on the concentration of free ligand available [*L*]. The black line corresponds to total added ligand in the absence of protein or receptor. In the simulations, $K_P = 1\,\mu M$, $K_R = 1$ nM and $[R]_T = 0.1$ nM.

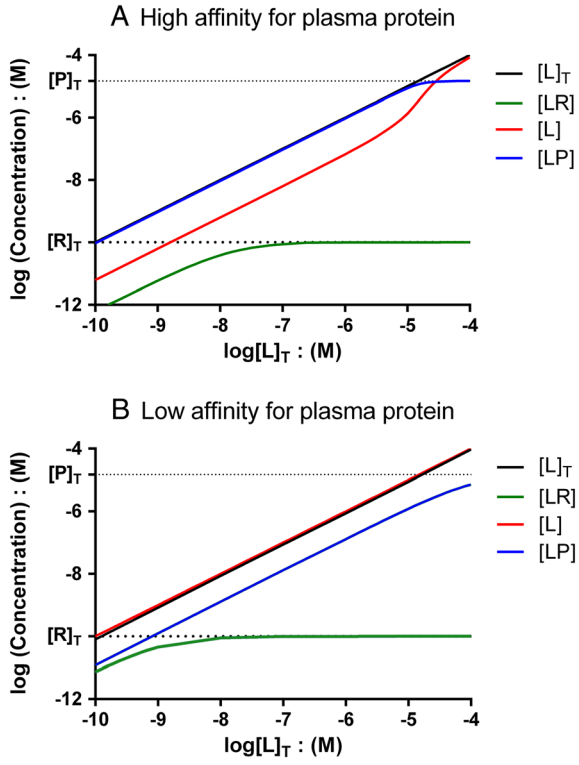

Figure 5

Comparing ligand–receptor and ligand–plasma protein occupancy simulations for compounds with high and low plasma protein affinity. (A) When ligand has a high affinity for plasma protein. Relationship between total ligand added and the concentrations of ligand bound to receptor, ligand bound to protein and free ligand for the parameter configurations $[P]_T = 15\,\mu M$, $K_R = 1$ nM, $K_P = 1\,\mu M$ and $[R]_T = 0.1$ nM. (B) When the ligand has a low affinity for plasma protein. Relationship between total ligand added and the concentrations of ligand bound to receptor, ligand bound to protein and free ligand for the same parameter configurations as (A), except $K_P = 100\,\mu M$.

and that the free ligand [*L*] is only approximately equal to the total ligand added, for the given parameter configurations, at a concentration approaching 100 μM. What is clear is that there is a steep shift in the free ligand corresponding to the incomplete saturation of protein. Figure 5B has the same parameter configurations as those in Figure 5A barring a lower affinity of the ligand for the protein, namely $K_P = 100\,\mu M$. This configuration results in full saturation of receptor at lower concentrations of ligand added, as one would expect, because proportionally more free ligand is available for any concentration of ligand added.

Using binding models to estimate plasma protein affinity (K_P)

As a consequence of formulating an analytical solution equation 10 that describes ligand binding in the presence of protein, it is now possible to use least-squares regression to provide protein affinity estimates (K_P) by programming the explicit solution of the cubic equation into statistical packages such as PRISM (detailed in Appendix 2).

We also explored the possibility of using an analysis similar in principle to Schild analysis to determine the affinity of ligand for plasma protein (Arunlakshana and Schild, 1959). Classically, Schild analysis is used to calculate the affinity of an antagonist for its receptor in the presence of an agonist by making use of a Schild plot, constructed from agonist dose ratios (DR) calculated for several concentrations of competing antagonist (Kenakin, 1982; Kenakin, 1992). The logarithm of these DR minus 1 ($\log(DR-1)$) is then plotted against the log of the concentration of the antagonist, and the data are fitted using linear regression. Mathematically, DR are defined through the equations derived by Gaddum to calculate fractional receptor occupancy (f) of agonist in the presence of antagonist (Gaddum, 1937). Our intention here is to show that, given the explicit solution to the cubic provided in Equation 10, one can use Schild analysis to calculate the affinity of the ligand for the protein; see Appendix 4 for full derivation. To this end, we modelled ligand–receptor occupancy, using the explicit solution to the cubic, keeping receptor concentration, ligand–protein affinity and ligand–receptor affinity fixed while varying protein and total ligand concentration as shown in Figure 6A. Using the same principles governing Schild analysis, we calculated DR from these ligand–receptor occupancy plots and plotted (y-axis) them against plasma protein concentration (x-axis) rather than antagonist concentration as is the norm. The affinity of ligand for the protein is reflected in the intercept on the x-axis of the Schild plot (Figure 6B) (i.e. $K_P = 1\ \mu M$).

It should be noted that Schild analysis can fail to provide a reliable estimate for K_P when the affinity for the protein is greater than that for the receptor, i.e. $K_R > K_P$ and $[P]_T < [L]_T$. This situation is, however, seldom seen as molecules in a lead optimization programme often have a higher affinity for their target than the micromolar range commonly observed for plasma proteins. The situation $K_R > K_P$ results in a change of root in the explicit solution to the cubic; namely instead of considering the solution as given in Equation 10 for $[LR]$, the requisite root is given by $[LR] = 2\sqrt{\frac{-q}{3}}\cos\left(\frac{\theta+4\pi}{3}\right) - \frac{a}{3}$ with the same parameter values for the coefficients in the cubic.

As simulated in Figure 7, for situations in which the protein affinity exceeds the receptor affinity, the binding curves become non-parallel in nature and hence are not suitable for the Schild-type analysis.

Testing the Schild method experimentally. In order to demonstrate that the Schild-type method was applicable in practice, we used a prostacyclin IP receptor binding assay as a model system. We constructed saturation curves to the radiolabelled IP receptor-antagonist [^{3}H]-RO-1138452 in the absence and presence of increasing concentrations of HSA (Figure 8). Specific [^{3}H]-RO-1138452 binding to CHO-IP membranes was saturable and best described by the interaction of the radioligand with a single population of high-affinity binding sites. The IP receptor expression level of the CHO-IP cell line was estimated from the B_{max} in [^{3}H]-RO-1138452 saturation binding as 10.01 ± 0.57 pM mg^{-1} ($n = 10$). From these studies, the equilibrium dissociation constant (K_d) of [^{3}H]-RO-1138452 was determined to be 0.22 ± 0.03 nM ($n = 10$). Upon the addition of increasing concentrations of HSA to the assay (Figure 8A), a parallel rightward shift in the saturation curve was observed with no significant reduction in the B_{max}. In order to estimate the pK_P value of [^{3}H]-RO-1138452 for HSA, the $\log(DR-1)$ was calculated for the binding at each concentration of HSA

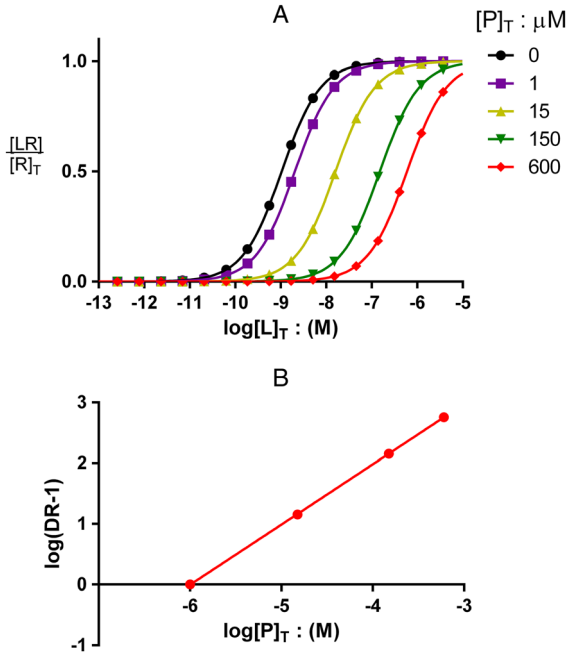

Figure 6

Schild analysis can be used to determine ligand–protein affinity estimates using binding data. (A) Simulation of the effects of increasing the concentration of protein on the concentration of ligand bound to receptor for the parameter configuration $K_R = 1$ nM, $K_P = 1\ \mu M$ and $[R]_T = 0.1$ nM. (B) Schild plot constructed by calculating dose ratios (DR) from the ligand–receptor occupancy plot. The affinity for the protein can be determined from the intercept on the x-axis, $K_P = 10^{-6}$ M or $K_P = 1\ \mu M$.

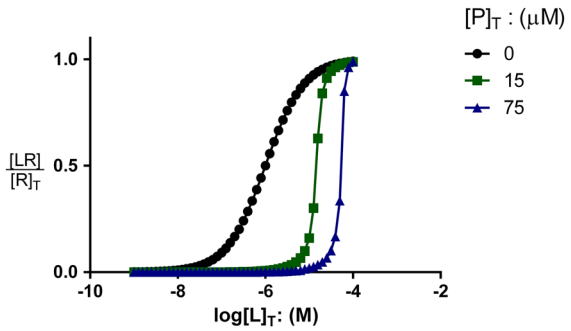

Figure 7

Situations where the affinity for protein exceeds the affinity for the receptor. Simulation of the effects of increasing the concentration of protein on the concentration of ligand bound to receptor. Parameter configurations are $K_P = 0.1\ \mu M$, $K_R = 1\ \mu M$ and $[R]_T = 0.1$ nM.

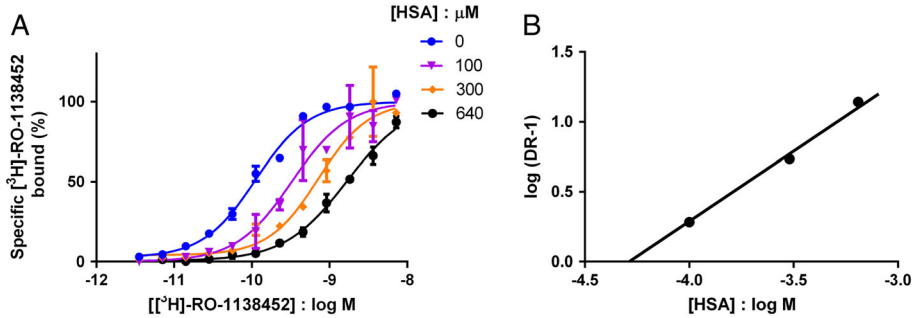

Figure 8

Practical application of Schild analysis to a radioligand binding assay. Saturation binding of [^{3}H]-RO-1138452 to CHO-IP cell membranes in the presence of increasing concentrations of HSA with corresponding Schild plot. (A) Increasing concentrations of [^{3}H]-RO-1138452 were incubated with CHO-IP cell membranes (2.5 μg per well) and the indicated concentrations of SA (HSA) at room temperature. As the total binding varied, data are shown as mean ± range from a representative of at least three independent experiments performed in duplicate and plotted as the percentage of specific bound. (B) For each set of experiments, the mean of the data at each SA concentration was taken, and the log(DR − 1) calculated. A Schild plot was constructed from these data using a first-order polynomial (straight line) equation, with slopes not significantly different from unity, from which pK_P values of [^{3}H]-RO-1138452 for HSA were determined from the intercept at the *x*-axis.

tested and plotted against the log of the HSA concentration to produce a Schild plot (Figure 8B). Individual Schild slopes from three independent experiments performed in duplicate were not significantly different from unity (0.96 ± 0.10), and therefore, slopes were constrained to unity. A mean pK_P value for [^{3}H]-RO-1138452 binding to HSA was estimated from the *x*-axis intercept values of these Schild plots, which was found to be 4.19 ± 0.17 (or a K_P of 65 μM).

In order to compare this value with one derived using a more conventional method, we utilized RED to assess the fraction of RO-1138452 bound to plasma. By comparing the concentration of drug in the buffer cell with that found in the plasma side, the percentage of bound drug in plasma was calculated to be 95.2 ± 0.41% (n = 3). Using the equation described by Toutain and Bousquet-Melou (2002), this value was used to estimate the K_P of RO-1138452 in plasma of 33 μM. This value compares well with the K_P calculated for serum albumin using the [^{3}H]-RO-1138452 binding assay (65 μM), suggesting that the main component in plasma that binds RO-1138452 is serum albumin and that the Schild-type method is an accurate way of assessing compound affinity at individual plasma proteins.

Simulating functional assays

Incorporating an operational model. Using the binding equations described above, it is possible experimentally to estimate the affinity of radiolabelled ligands for plasma protein. However, it is not practical to radiolabel every compound of interest in order to obtain accurate protein affinity values. We, therefore, explored the possibility of utilizing functional assays for the estimation of K_P values. A pragmatic model relating binding and function has been previously described by Black and Leff (1983) who constructed an operational model of agonism describing the efficacy of agonists and partial agonists once bound to receptors. Starting from the Hill–Langmuir equation, they derived the so-called transducer function, a function describing the transduction of receptor occupation into a response

$$E = \frac{E_m \cdot [AR]}{K_E + [AR]} \tag{11}$$

where $[AR]$ is the concentration of agonist bound to receptor, K_E is the concentration of $[AR]$ that elicits 50% maximal response and E_m is the maximum response possible in the system under study. Using our explicit equation for the concentration of ligand bound to receptor equation 10, we can generate operational model curves for different K_E values using equation 11 in the presence and absence of plasma protein $[P]_T$ within the cubic model, as simulated in Figure 9A and B. The inclusion of plasma protein produces the expected rightward shift of the agonist $[L]_T$ effect curve but has no apparent effect on the maximal agonist response. This is analogous to the effect of including plasma protein in a saturation binding experiment, as illustrated in Figure 2B. Also demonstrated in this model is the graded reduction in agonist effect and potency as one increases the value of K_E, as expected in the operational model.

We have utilized this operational form of the model to simulate a Schild-type analysis, as described above for binding experiments. As can be seen from Figures 10A and 9B, this suggests that Schild-type analysis can be used in functional assays to determine the affinity of a compound for serum protein.

Discussion

Plasma protein binding is an important parameter in many drug discovery projects and is usually measured using equilibrium dialysis, ultrafiltration or liquid chromatography techniques. While these approaches are sufficient for the large majority of compounds, they can struggle to differentiate between ligands that are >99.5% bound. In order to

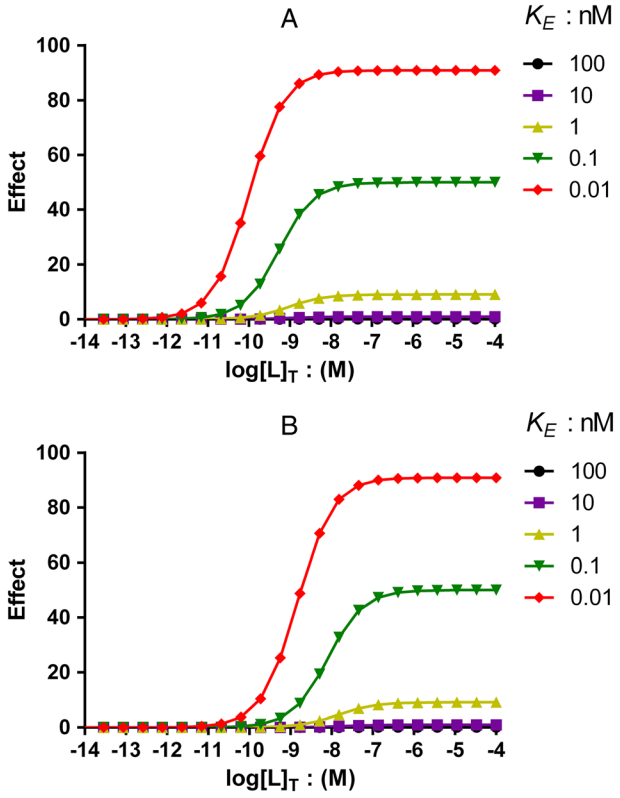

Figure 9

Simulations showing the effect of including plasma proteins in a functional assay using operational modelling. Effect of changing the parameter K_E on functional effect curves. (A) In the absence of plasma protein (parameter values $K_R = 1$ nM, $K_P = 1$ μM, $[R]_T = 0.1$ nM and $E_{max} = 100$) and (B) with total protein $[P]_T$ fixed at 15 μM for the same parameter values as defined above.

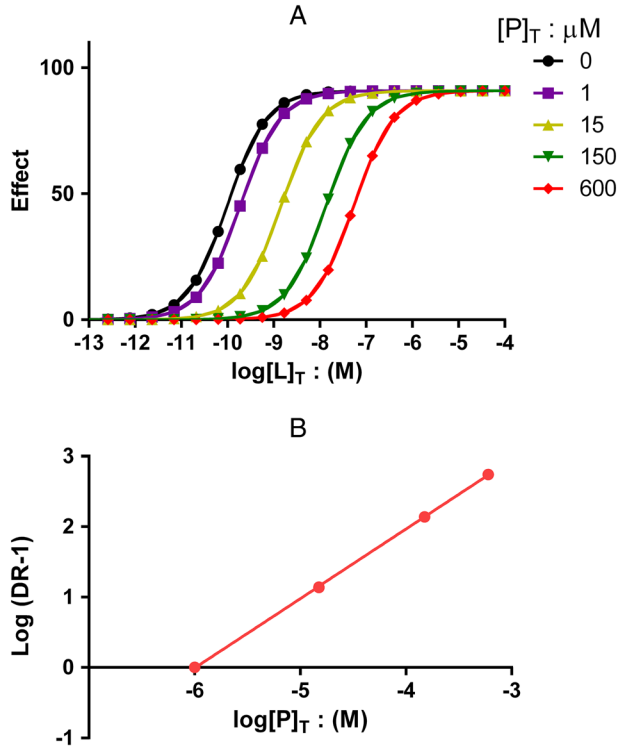

Figure 10

Schild analysis can be used to determine ligand–protein affinity estimates from functional data. (A) Operational model with increasing concentrations of protein for the parameter configurations $K_P = 1$ μM, $K_E = 10$ pM, $K_R = 1$ nM, $[R]_T = 0.1$ nM and $E_{max} = 100$. (B) The resulting Schild plot shows that the affinity for the protein can be determined from the intercept on the x-axis, $K_P = 10^{-6}$ M or $K_P = 1$ μM.

discriminate between highly bound compounds, it becomes necessary to consider binding in terms of equilibrium affinity constants rather than fraction bound. A theoretical model for predicting serum albumin affinities utilizing an IC_{50} shift assay has been described by Copeland (2000). We have expanded this principle to create a thermodynamically complete model at equilibrium considering conservation of mass for each species. This model has two main utilities. Firstly, it can be used to explore the potential influence of plasma proteins on observed pharmacology in *in vitro* assays, and secondly, it can be employed to determine the affinity of compounds at plasma proteins, using either direct fitting to data or by the commonly used Schild plot. The model is in the form of a cubic equation with coefficients given in terms of concentrations of total ligand, receptor and protein added, and incorporating their associated equilibrium dissociation constants K_R and K_P. By ensuring conservation of each species, we can explore depletion of each component in the system, which is evident in a number of the simulations we have performed.

These simulations illustrate how the inclusion of plasma protein directly affects the position of the saturation curve; if a ligand has affinity for serum protein, then inclusion of that protein in an *in vitro* assay would result in an underestimation of the affinity at the receptor. This is of particular importance as it is often routine to include serum albumin in *in vitro* assays to reduce non-specific binding of compounds, especially radioligands. In addition, we have simulated binding curves of ligand bound to protein for various values of K_P and simulated concentrations of free ligand for various concentrations of protein with a fixed K_P, highlighting the dramatic effect protein can have on the concentration of free drug. This free drug fraction can be considered proportional to the total added ligand concentration over a large concentration range, but our simulations demonstrate that a deviation from this linear relationship will occur once the concentration of drug exceeds the concentration of plasma protein to which it binds. While this is highly unlikely to occur for the majority of clinically used drugs *in vivo*, it could become a significant issue in an *in vitro* assay system where significantly less protein is added. For example, routinely utilized serum albumin concentrations range from 1.5 to 15 μM (0.01–0.1%), concentrations that are often exceeded for compounds in *in vitro* biochemical assays.

Although it is beneficial to consider the influence of plasma proteins on direct binding of ligand to receptor, it

is becoming more common to utilize functional assays to characterize new compounds. To address this, we have incorporated our explicit solution for the ligand–receptor complex into the operational model of pharmacological agonism (Black and Leff, 1983) to enable simulation and analysis on functional responses in the presence and absence of plasma proteins. As can be seen from the simulations, these equations behave as predicted for an operational model, with changes in agonist efficacy ($1/K_E$ in our model) resulting in a shift in maximal response and/or agonist potency. Importantly, although the inclusion of plasma protein can affect apparent potency of an agonist, it is not able to change the maximal response at saturating concentrations of ligand.

In addition to these simulations, we have considered a number of methods for determining plasma protein affinities for compounds, which can potentially be employed in membrane or cell-based binding and functional assays. In order to determine K_P, it is possible to either directly fit experimental data to the cubic equation or perform utilize Schild analysis, where binding (or function) curves are constructed in the presence of increasing concentrations of plasma protein. Indeed, Schild analysis might be preferred, particularly when directly fitting functional data where estimation of K_R and K_E might be challenging (Kenakin *et al.*, 2012). We have demonstrated using the prostacyclin IP receptor as a model system that this method can be applied to experimental radioligand binding data and that the resulting K_P was comparable with that obtained using a more conventional method to determine drug binding to plasma proteins.

Although this model can be very useful in determining affinity of compounds to serum proteins, there are a number of limitations that should be addressed. It is important to highlight that we have taken a reductionist approach, with the mathematical equations presented here only modelling the scenario where the drug binds to a single site on the plasma protein. As discussed in Trainor (2007) and Sjöholm *et al.* (1979), it is known that there are multiple binding sites on HSA, two of which are thought to predominate, designated site I, the warfarin binding site, and site II, the indole-benzodiazepine site (Sudlow *et al.*, 1975). Site I is thought to bind mainly heterocyclic and negatively charged compounds, whereas site II prefers small aromatic carboxylic acids. Although it would be possible to extend this analysis to incorporate two binding sites on HSA, a similar approach to the one we have used to reduce the equilibrium equations to a single equation in $[LR]$ results in a quartic equation. While the analytic solution of a quartic equation can be found, it is very complicated, and so, in practice, it would be better to solve the equation numerically for given parameter values. It should also be highlighted that the theoretical framework presented in this paper is applicable only to *in vitro* studies measuring affinity to a single plasma protein at any one time and will not directly model the effect *in vivo* due to an increased number of additional proteins in blood. Finally, it is important to ensure that the assay system can tolerate variable concentrations of plasma protein. In some systems, inclusion of high concentrations of serum may deplete other important molecules, such as cofactors or substrates required for enzymatic assays. Conversely, in signalling assays, the exclusion of plasma protein may reduce cell viability over extended periods of time, complicating the interpretation of results. It is therefore critical to establish the sensitivity of the assay to variable plasma protein concentrations, which may limit the practical application of this method (also discussed by Rusnak *et al.*, 2004).

In summary, the model described here enables exploration of the impact of plasma proteins in simple assay systems and also provides several approaches to quantify the affinity of compounds for serum proteins. Importantly, it is possible to apply these approaches to commonly used biochemical assays, enabling differentiation of highly bound compounds (>99.5%) at an early stage of the drug discovery process, ultimately resulting in a better understanding of the structure–activity relationship for plasma protein binding.

Acknowledgements

We are grateful to Dr Gianne Derks for some helpful discussions concerning this work. This work was funded by Novartis Institutes for Biomedical Research. Blakely was partly funded by a Universities of Reading and Surrey Biopharma Graduate Internship award.

Author contributions

D.B., D.A.S., P.E., E.B., P.J.A. and S.J.C. performed the research and analysed the data. S.J.C. designed the research study. D.B., D.A.S., E.B., P.J.A. and S.J.C. wrote the paper.

Conflict of interest

None.

References

Alexander SPH, Benson HE, Faccenda E, Pawson AJ, Sharman JL, Spedding M *et al.* (2013). The Concise Guide to PHARMACOLOGY 2013/14: G protein-coupled receptors. Br J Pharmacol. 170: 1459–1581.

Arunlakshana O, Schild HO (1959). Some quantitative uses of drug antagonists. Br J Pharmacol 14: 48–58.

Black JW, Leff P (1983). Operational models of pharmacological agonism. Proc R Soc Lond B 220: 141–162.

Carter CM *et al.* (2007). Miniaturized receptor binding assays: complications arising from ligand depletion. J Biomol Screen 12: 255–266.

Copeland RA (2000). Determination of serum protein binding affinity of inhibitors from analysis of concentration–response plots in biochemical activity assays. J Pharm Sci 89: 1000–1007.

Gaddum JH (1937). The quantitative effects of antagonistic drugs. J Physiol 89: 7–9.

Goldstein A, Barrett RW (1987). Ligand dissociation constants from competition binding assays: errors associated with ligand depletion. Mol Pharm 31: 603–609.

Goodman LS, Gilman AG (1996). The Pharmacological Basis of Therapeutics, 19th edn. New York: McGraw-Hill.

Kenakin TP (1982). The Schild regression in the process of receptor classification. Can J Physiol Pharm 60: 249–265.

Kenakin TP (1992). Tissue response as a functional discriminator of receptor heterogeneity: effects of mixed receptor populations on Schild regressions. Mol Pharm 41: 699–707.

Kenakin T, Watson C, Muniz-Medina V, Christopoulos A, Novick S (2012). A simple method for quantifying functional selectivity and agonist bias. ACS Chem Neurosci 21: 193–203.

Kratochwil NA, Huber W, Muller F, Kansy M, Gerber PR (2002). Predicting plasma protein binding of drugs: a new approach. Biochem Pharmacol 64: 1355–1374.

Meserve BE (1982). Fundamental Concepts of Algebra. Dover: New York.

Pawson AJ, Sharman JL, Benson HE, Faccenda E, Alexander SP, Buneman OP *et al.* (2014). The IUPHAR/BPS Guide to PHARMACOLOGY: an expert-driven knowledgebase of drug targets and their ligands. Nucl. Acids Res. 42 (Database Issue): D1098–106.

Rusnak DW *et al.* (2004). A simple method for predicting serum protein binding of compounds from IC_{50} shift analysis for *in vitro* assays. Bioorg Med Chem Lett 14: 2309–2312.

Sjöholm I, Ekman B, Kober A, Ljungstedt-Påhlman I, Seiving B, Sjödin T (1979). Binding of drugs to human serum albumin XI. The specificity of three binding sites as studied with albumin immobilized in microparticles. Mol Pharm 16: 767–777.

Sudlow G, Birkett DJ, Wade DN (1975). The characterization of two specific drug binding sites on human serum albumin. Mol Pharm 11: 824–832.

Sykes DA, Dowling MR, Charlton SJ (2009). Exploring the mechanism of agonist efficacy: a relationship between efficacy and agonist dissociation rate at the muscarinic M3 receptor. Mol Pharm 76: 543–551.

Toutain PL, Bousquet-Melou A (2002). Free drug fraction vs. free drug concentration: a matter of frequent confusion. J Vet Pharmacol Therap 25: 460–463.

Trainor GL (2007). The importance of plasma protein binding in drug discovery. Expert Opin. Drug Discovery 2: 51–64.

Waters NJ, Jones R, Williams G, Sohal B (2008). Validation of a rapid equilibrium dialysis approach for the measurement of plasma protein binding. J Pharmaceut Sci 97: 4586–4595.

Weisstein EW (n. a) Cubic formula. From MathWorld – A Wolfram Web Resource. http://mathworld.wolfram.com/CubicFormula.html.

Wells JW, Birdsall NJ, Burgen AS, Hulme EC (1980). Competitive binding studies with multiple sites: effects arising from depletion of the free radioligand. Biochim Biophys Acta 632: 464–469.

Appendix 1

From a mathematical perspective, Equation (8) is only valid when $[LR] \neq [R]_T$, and here, we show how this must be the case. We assume that $[R]_T \neq 0$, and we want to show that any solution of Equations 1–5 must satisfy $[LR] \neq [R]_T$. To do this, assume the contrary, namely that $[LR] = [R]_T$. In this case, it follows from 5 that $[R] = 0$ and substituting $[LR] = [R]_T$ and $[R] = 0$ into 1 that $K_R = 0$. However, this is not the case, which implies that our original assumption must be incorrect, and so, $[LR] \neq [R]_T$.

Appendix 2

The cubic equation that we are considering is given by

$$Ax^3 + Bx^2 + Cx + D = 0 \tag{A1}$$

where

$$A = K_R - K_P$$
$$B = K_P K_R + 2\,K_P[R]_T + K_P[L]_T + K_R[P]_T - K_R^2 - K_R[L]_T - K_R[R]_T$$
$$C = [R]_T\left(-K_P K_R - K_P[R]_T - 2\,K_P\,[L]_T - K_R[P]_T + K_R[L]_T\right)$$
$$D = K_P[L]_T[R]_T^2$$

In lead optimization programs, it is almost always the case that the affinity of a compound for the receptor is higher than that for plasma protein, so if we assume that $K_P > K_R$ then we note that $A\langle 0,\ B\rangle 0,\ C\langle 0,\ D\rangle 0$. Using Descartes' rule of signs (Meserve, 1982), it follows that the cubic equation A1 has zero negative roots and either one or three positive roots. Clearly, if there is only one positive root, then the other two roots must be complex. Using the equation for $[L]_T$ as given in 11, namely

$$[L]_T = \big[[LR]K_P K_R[R]_T - K_P K_R[LR] - 2K_P[R]_T[LR] + K_P[LR]^2 + K_R[P]_T[R]_T + K_P[R]_T^2 + K_R^2[LR] - K_R[LR][P]_T - K_R[LR]^2 + K_R[LR][R]_T\big]/([R]_T - [LR])\left(-K_P[LR] + K_R[LR] + K_P[R]_T\right) \tag{A2}$$

and assuming that K_R, K_P, $[R]_T \neq 0$, it can be shown that

$$lim_{[LR]\to 0}\,[L]_T = 0\,,\quad lim_{[LR]\nearrow[R]_T}\,[L]_T = \infty,\ 0 < \frac{d[L]_T}{d[LR]} < \infty \text{ if } 0 < [LR] < [R]_T$$

The last result on the derivative can be shown by considering separately the numerator and denominator of the derivative. The denominator is zero when $[LR] = [R]_T$ but is non-zero in the given range for $[LR]$. The numerator is a quartic function of $[LR]$. Descartes' rule of signs (Meserve, 1982) can be used to show that this quartic has no roots with $[LR] < [R]_T$, and hence, there are no sign changes of the derivative in the given interval, as claimed.

It follows immediately from these results that, for a given $[L]_T$ (with $0 \le [L]_T < \infty$), there is precisely one solution of the cubic equation A1 with $0 \le [LR] < [R]_T$, and because the cubic equation has no negative roots, this must be the smallest root of the cubic.

The solutions of the cubic equation A1 can be found (Weisstein, n.a) by first dividing the equation by A, giving

$$x^3 + ax^2 + bx + c = 0$$

where $x = [LR],\ a = \frac{B}{A}\,,\ \ b = \frac{C}{A}\,,\ \ c = \frac{D}{A}$

We define the parameters

$$q = \frac{3b - a^2}{3}\ ,\quad r = \frac{2a^3 - 9ab + 27c}{27},\qquad d = \frac{q^3}{27} + \frac{r^2}{4}$$

The solutions of the cubic can be classified by the value of the parameter d. In particular,

Case 1: $d = 0$: three real roots – two equal,

$$x_1 = 2\left(\frac{-r}{2}\right)^{1/3} - \frac{a}{3}$$

$$x_2 = x_3 = -\left(\frac{-r}{2}\right)^{1/3} - \frac{a}{3}$$

Case 2: $d > 0$: one real root and

$$x_1 = \left(-\frac{r}{2} + d^{1/2}\right)^{1/3} + \left(-\frac{r}{2} - d^{1/2}\right)^{1/3} - \frac{a}{3}$$

Case 3: $d < 0$: three real roots

$$x_1 = 2\sqrt{\frac{-q}{3}}\cos\left(\frac{\theta}{3}\right) - \frac{a}{3}$$

$$x_2 = 2\sqrt{\frac{-q}{3}}\cos\left(\frac{\theta + 2\pi}{3}\right) - \frac{a}{3}$$

$$x_3 = 2\sqrt{\frac{-q}{3}}\cos\left(\frac{\theta + 4\pi}{3}\right) - \frac{a}{3}$$

where $\theta = \cos^{-1}\left(\left(\frac{3r}{2q}\right)\cdot\sqrt{\frac{-3}{q}}\right)$.

All the examples that we consider have $d < 0$, and hence, there are three real roots to the cubic. The analysis given earlier showed that we require the smallest of the roots, and it can be verified that this is the root x_2.

To facilitate the practical application of this solution, it is presented later in PRISM language:

Y corresponds to the complex $[LR]$.

K_R is the equilibrium dissociation constant for the ligand binding to receptor.

K_P is the equilibrium dissociation constant for the ligand binding to protein.

X is the total added ligand concentration given in log units.

Rtot is the total added receptor concentration.

Ptot is the total added protein concentration.

```
a = (KP*KR + 2*KP*Rtot + KP*10^X
   + KR*Ptot − KR*KR − KR*10^X − KR*Rtot)/(KR − KP)
b = (Rtot*(−KP*KR − KP*Rtot − 2*KP*10^X − KR*Ptot
   + KR*10^X))/(KR − KP)
c = (KP*10^X*Rtot^2)/(KR − KP)
q = (3b − a^2)/3
r = (2*a^3 − 9*a*b + 27*c)/27
d = q^3/27 + r^2/4
theta = arccos(((3*r)/(2*q))*sqrt(−3/q))
Y = 2*sqrt(−q/3)*cos((theta + 2*Pi)/3) − a/3
```

Appendix 3: Explicit solution of [*LP*] and [*L*]

Solution of [LP]:

By suitable manipulation of Equations 4–7, one can also derive cubic equations for the concentrations of ligand bound to protein and free ligand. The explicit cubic expression for the concentration of ligand bound to protein in this scenario is

$$E[LP]^3 + F[LP]^2 + G[LP] + H = 0$$

where

$$E = K_P - K_R$$
$$F = K_P K_R + 2\,K_R[P]_T + K_R[L]_T + K_P[R]_T - K_P^2 - K_P[L]_T - K_P[P]_T$$
$$G = -K_P K_R[P]_T - K_R[P]_T^2 - 2\,K_R\,[L]_T[P]_T - K_P[P]_T[R]_T + K_P[L]_T[P]_T$$
$$H = K_R[L]_T[P]_T^2$$

One can perform a similar analysis as used previously to determine the physiologically relevant root, but in this case, the variables a, b and c are defined by $a = F/E$, $b = G/E$ and $c = H/E$. The variables q, r and θ are then defined as in Appendix 2. For our purposes, the relevant root is given by

$$[LP] = 2\sqrt{\frac{-q}{3}}\cos\left(\frac{\theta + 4\pi}{3}\right) - \frac{a}{3}$$

Solution of [*L*]:

The final quantity to consider in the problem is the free concentration of ligand remaining after all the interactions. Again, one can formulate a cubic equation of the form

$$J[L]^3 + K[L]^2 + M[L] + N = 0$$

where

$$J = -1$$
$$K = [L]_T - [R]_T - K_R - K_P - [P]_T$$
$$M = K_P[L]_T + K_R[L]_T - K_P[R]_T - K_R[P]_T - K_P K_R$$
$$N = K_R K_P[L]_T$$

to quantify this concentration in terms of the known parameters.

In this case, since $J = -1$, we have the new definitions $a = -K$, $b = -M$ and $c = -N$. As before, the variables q, r and θ are then defined as in Appendix 2. The physiologically relevant root is found to be $[L] = 2\sqrt{\frac{-q}{3}}\cos\left(\frac{\theta}{3}\right) - \frac{a}{3}$.

Appendix 4

We are considering the situation where the receptor and protein compete to bind to the ligand:

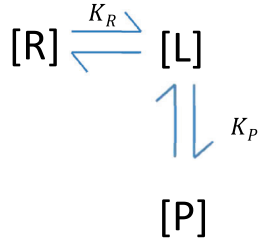

At equilibrium, Equations 1 and 2 hold. Using Equations 1 and 5, we obtain

$$\frac{[LR]}{[R]_T} = \frac{\frac{1}{K_R}[L][R]}{[R] + [LR]} = \frac{\frac{1}{K_R}[L][R]}{[R] + \frac{1}{K_R}[L][R]} = \frac{\frac{1}{K_R}[L]}{1 + \frac{1}{K_R}[L]} \qquad \text{(A2)}$$

Now, using Equations (1–3), we have

$$[L]_T = [L] + [LR] + [LP] = [L] + \frac{1}{K_R}[L][R] + \frac{1}{K_P}[L][P]$$
$$= [L]\left(1 + \frac{1}{K_R}[R] + \frac{1}{K_P}[P]\right)$$

Hence, $[L] = \frac{[L]_T}{\left(1+\frac{1}{K_R}[R]+\frac{1}{K_P}[P]\right)} = \frac{[L]_T K_R K_P}{(K_R K_P + K_P[R] + K_R[P])}$ ∂ and substituting into (A2) gives the response

$$\frac{[LR]}{[R]_T} = \frac{[L]_T K_P}{(K_R K_P + K_P[R] + K_R[P])\left(1 + \frac{[L]_T K_P}{K_R K_P + K_P[R] + K_R[P]}\right)}$$
$$= \frac{[L]_T K_P}{K_R K_P + K_P[R] + K_R[P] + [L]_T K_P}$$

Considering no protein (i.e. $[P] = 0$) and denoting the free and bound concentrations with a prime, we have the response

$$\frac{[LR]'}{[R]_T} = \frac{[L]_T K_P}{K_R K_P + K_P[R]' + [L]_T K_P}$$

For equal responses with and without inclusion of protein (i.e. $[LR]' = [LR]$), it follows from 5 that $[R] = [R]'$, and then

$$\frac{[L]'_T K_P}{K_R K_P + K_P[R] + K_R[P] + [L]'_T K_P} = \frac{[L]_T K_P}{K_R K_P + K_P[R] + [L]_T K_P}$$

Defining $DR = [L]'_T/[L]_T$ and solving for DR provides the following solution:

$$DR = \frac{K_R K_P + K_P[R] + K_R[P]}{K_P(K_R + [R])}$$

which can be simplified and rearranged as follows:

$$DR - 1 = \frac{K_R[P]}{K_P(K_R + [R])}$$

Taking logs then gives

$$\log(DR - 1) = \log[P] - \log K_P + \log\left(\frac{K_R}{K_R + [R]}\right) \qquad \text{(A3)}$$

This implies that $[R]$ affects the Schild analysis by the factor $\log\left(\frac{K_R}{K_R+[R]}\right)$. Note, however, that when $[R] \ll K_R$, then $[R]/K_R \ll 1$, and so,

$$\log\left(\frac{K_R}{K_R + [R]}\right) = \log\left(\frac{1}{1 + [R]/K_R}\right) = -\frac{[R]}{K_R} + O\left(\left(\frac{[R]}{K_R}\right)^2\right)$$

Thus, assuming that $[R]/K_R$ is negligible compared with $\log K_p$, then we can simplify A3 to

$$\log(DR - 1) = \log[P] - \log K_P$$

which gives the linear relationship between $\log(DR - 1)$ and $\log[P]$ from which the constant K_P can be found.